*Journal of*
*Nanoscience and Nanotechnology*
Vol. 11, 1373–1376, 2011

# Efficient Phosphorescent Green and Red Organic Light-Emitting Diodes Based on the Novel Carbazole-Type Host Material

Ji Hyun Seo[1], Hoe Min Kim[1], Eun Young Choi[1], Dae Hyuk Choi[2], Jung Hwan Park[2], Kum Hee Lee[3], Seung Soo Yoon[3,*], and Young Kwan Kim[1,*]

[1] *Department of Information Display, Hongik University, Seoul 121-791, Korea*
[2] *Corporate R&D center, Duksan Hi-Metal Co., Ltd., Seongnam 463-420, Korea*
[3] *Department of Chemistry, Sungkyunkwan University, Suwon 440-746, Korea*

We developed a novel carbazole-type material, 9-phenyl-3,6-bis(4-(1-phenyl-1H-benzo[d]imidazol-2-yl)phenyl)-9H-carbazole (LPGH 153), and fabricated the green and red phosphorescent organic light-emitting diodes (OLEDs) using LPGH 153 as host. The red and green devices have the max. luminous efficiencies of 22.2 cd/A and 32.2 cd/A, respectively.

**Keywords:** Carbazole-Type Host, Organic Light-Emitting Diode, Green, Red.

## 1. INTRODUCTION

In the last decade, efforts have been devoted to the development of materials useful for the fabrication of organic light-emitting diodes (OLEDs).[1–2] The OLED performance was found to depend not only on the luminescence efficiency of the emissive materials but equally importantly also on the optical and semiconductor characteristics of hosts and charge-transporting materials. Because of the multiplicity of factors influencing these features, molecular design of such materials is fairly complicated as it requires optimizing properties that include the highest occupied molecular orbital (HOMO)—the lowest unoccupied molecular orbital (LUMO) levels, triplet excited states energy levels, film forming behavior, thermal stability, and suitable emission wavelength. Phosphorescent OLEDs employing phosphorescent emitters doped into a proper charge transporting host material have attracted significant attention because of their high efficiencies as a consequence of the utilization of both singlet and triplet excitons.[3] In most studies, the phosphorescent dopant materials were doped into a common 4,4′-bis(N-carbazolyl)biphenyl (CBP) host material.[4–9] However, the driving voltage of the CBP based device was rather high and the quantum efficiency was not improved in the CBP based devices. In addition to CBP host, bis(2-methyl-8-quinolinolato)(biphenyl-4-olato)aluminium was used as a host for phosphorescent device and high efficiency, stable lifetime and low driving voltage were observed.[10] Recently, Kanno et al. reported Zn based organometallic complexes as host materials to reduce the driving voltage of OLEDs.[11] In this work, a novel carbazole-type compound, 9-phenyl-3,6-bis(4-(1-phenyl-1H-benzo[d]imidazol-2-yl)phenyl)-9H-carbazole (LPGH 153), was developed and the device performances of the red and green phosphorescent OLED with the LPGH 153 was investigated.

## 2. EXPERIMENTAL DETAILS

### 2.1. Synthesis of LPGH 153

### *2.1.1. Synthesis of 3,6-Dibromo-9H-Carbazole (1)*

Carbazole (15 g, 90 mmol) was dissolved in anhydrous $CH_2Cl_2$ (250 mL) and added of *N*-bromosuccinimide (NBS, 48 g, 270 mmol) at room temperature under nitrogen atmosphere. The mixture was stirred at room temperature for 6 h. After the reaction was done, the reaction mixture was quenched by addition of water. The crude was extraction with $CH_2Cl_2$ and washed with water. The combined organic layer was dried over anhydrous $MgSO_4$, filtered and concentrated under reduced pressure. The residue was purified by recrystallization with $CH_2Cl_2$ and hexane to obtain pure **1** (24.7 g, 85%) shown in Scheme 1. $^1$H NMR (400 MHz, $CDCl_3$): $\delta$ (ppm) 7.38 (d, 2H), 7.57 (dd, 2H), 8.12 (d, 2H), 8.31 (s, 1H, NH).

---

[*] Authors to whom correspondence should be addressed.

1533-4880/2011/11/1373/004

doi:10.1166/jnn.2011.3370

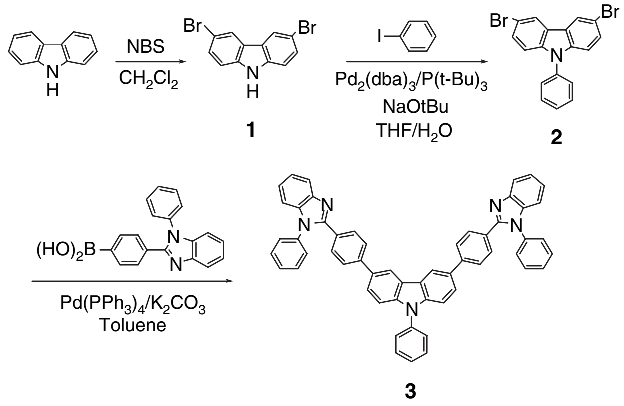

**Scheme 1.** Synthesis process of the LPGH 153.

### 2.1.2. *Synthesis of 3,6-Dibromo-9-Phenyl-9H-Carbazole (2)*

Iodobenzene (13.8 g, 67.7 mmol), $Pd_2(dba)_3$ (2.8 g, 3.1 mmol) and $P(t\text{-}Bu)_3$ (1.5 mL, 6.2 mmol) were added in THF (150 mL). Then, NaOtBu (14.8 g, 153.8 mmol) was dissolved in THF (50 mL) and water (50 mL), which was added as well. A solution of **1** (20 g, 61.5 mmol) in THF (50 mL) was slowly dropped into the reaction mixture and then refluxed for 12 h. After cooled to room temperature, the reaction mixture was filtered by Celite and extracted with $CH_2Cl_2$ and washed with water. The combined organic layer was dried over anhydrous $MgSO_4$, filtered and concentrated under reduced pressure. The residue was purified by column chromatography on $CH_2Cl_2$: hexane/3:1 as eluent solvents to obtain pure **2** (21 g, 75%) shown in Scheme 1. $^1$H NMR (400 MHz, $CDCl_3$): $\delta$ (ppm) 7.30 (d, 2H), 7.45 (m, 1H), 7.50 (d, 2H), 7.51 (dd, 2H), 7.58 (m, 2H), 8.07 (d, 2H).

### 2.1.3. *Synthesis of 9-Phenyl-3,6-Bis(4-(1-Phenyl-1H-Benzo[d]imidazol-2-yl)Phenyl)-9H-Carbazole (3)*

Iodobenzene (13.8 g, 67.7 mmol), $Pd_2(dba)_3$ (2.8 g, 3.1 mmol) and P(t-Bu 4-(1-Phenyl-1*H*-benzo[*d*]imidazol-2-yl)phenyl boronic acid (26.1 g, 83.1 mmol), $Pd(PPh_3)_4$ (1.9 g, 1.7 mmol), $K_2CO_3$ (11.5 g, 83.1 mmol) and **2** (25.9 g, 33.2 mmol) were successively added in toluene (200 mL) and then refluxed for 12 h. After cooled to room temperature, the reaction mixture was filtered by Celite and washed with hot toluene. After removed of organic solvent, the residue was purified by recrystallization with $CH_2Cl_2$ and hexane to obtain pure **3** (14.6 g, 53%) shown in Scheme 1. $^1$H NMR (400 MHz, $CDCl_3$): $\delta$ (ppm) 7.25–7.27 (m, 5H), 7.33–7.40 (m, 5H), 7.48–7.61 (m, 7H), 7.65 (d, 1H), 7.67 (d, 1H), 7.69 (m, 8H), 7.92 (m, 3H), 7.97–8.00 (m, 1H), 8.05 (d, 1H), 8.11 (d, 1H), 8.41 (d, 2H). $^{13}$C NMR (100 MHz, $CDCl_3$): $\delta$ (ppm) 110.35, 110.42, 118.88, 119.78, 123.00, 123.27, 124.08, 125.62, 126.92, 127.01, 127.54, 127.98, 128.08, 128.63, 129.87, 129.96, 130.05, 132.57, 137.17, 137.39, 141.23, 143.10, 152.25.

## 2.2. Device Fabrication

OLEDs were fabricated by high vacuum ($5 \times 10^{-7}$ torr) thermal evaporation of organic materials onto the surface of an indium tin oxide (ITO) coated glass substrate with resistance of 30 Ω/sq. The ITO glass was cleaned with acetone, methanol, distillated water, and isopropyl alcohol. And then the ITO was treated by $O_2$-plasma with power of 125 W for 2 minutes. The device configuration used in this work was ITO (150 nm)/4,4′,4″-tris[2-naphthylphenylamino]triphenylamine (2-TNATA) (60 nm)/4,4′-bis[N-(naphthyl)-N-phenyl-amino]biphenyl (NPB) (50 nm)/10% Ir complex doped LPGH 153 (30 nm)/bathocuproine (BCP) (20 nm)/tris-(8-hydroxyquinoline) aluminum ($Alq_3$) (30 nm)/lithium quinolate (Liq) (2 nm)/aluminum (Al) (100 nm). The iridium(III) tris(2-phenylpyridine) [$Ir(ppy)_3$] and iridium(III) bis(2-phenylquinoline) acetylacetonate [$Ir(pq)_2(acac)$] were used as phosphorescent green and red emitter, respectively. After the devices fabrication, the current density–voltage ($J$–$V$) characteristics of the OLEDs were measured with a source measure unit (Kiethley 236). The luminance and CIE chromaticity coordinates of the fabricated devices were measured using a chromameter (MINOLTA CS-1000).

## 3. RESULTS AND DISCUSSION

HOMO level of LPGH 153 was measured from cyclic voltammetry (CV) and the oxidation-reduction reaction as potential variation is shown in Figure 1. The HOMO level can be calculated from first oxidation peak in CV graph and electron energy level of reference electrode.[12] As a result, HOMO level of 5.9 eV was obtained. On the other hand, the band gap ($E_g$) of LPGH 153 was measured from absorption edge of UV/Vis. spectrum shown in inset of Figure 1 and it was 3.2 eV. Therefore, the LUMO level of 2.7 eV was obtained from difference between HOMO and $E_g$ of LGPH 153. Figure 2 shows the energy band diagram of device with LPGH 153. The LPGH 153 is suitable for exciton energy transfer from the LPGH 153 to red and green emitting $Ir(pq)_2(acac)$ and $Ir(ppy)_3$ with the $E_g$

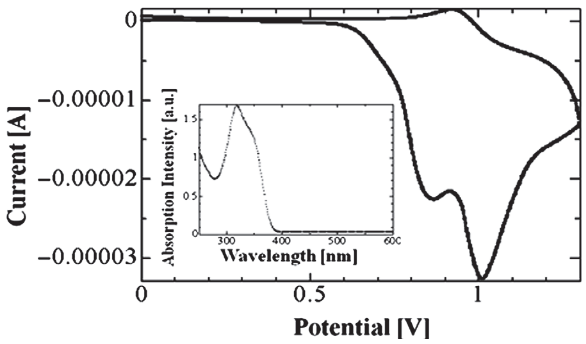

**Fig. 1.** Cyclic voltammetry (inset; UV/Vis. spectrum) of LPGH 153.

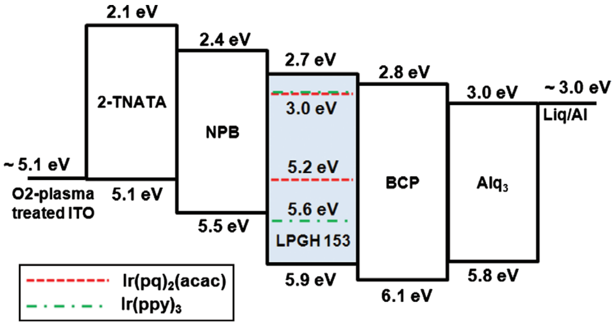

**Fig. 2.** Energy level diagram of the LPGH 153 device.

of 2.2 eV and 2.6 eV, respectively. Moreover, the HOMO and LUMO levels of LPGH 153 are suitable for injection of hole and electron and the carbazole unit is appropriate for balancing holes and electrons in the emitting layer. The electron transport property of the LPGH 153 was confirmed by the electron only devices and the LPGH 153 electron only device showed higher current density than the common CBP electron only device. In addition, the LPGH 153 host material forms an amorphous film with a surface roughness less than 1 nm due to its bulky molecular structure. Therefore, we expected that the LPGH 153 can be used as a host material for red and green phosphorescent OLEDs.

Figure 3 shows the current density–voltage curves of the red and green phosphorescent OLEDs with LPGH 153 host. The current density flow of red and green devices is similar, but the current density of green device is slightly higher than that of red device. It is because that the HOMO energy levels of Ir(pq)$_2$(acac) and Ir(ppy)$_3$ are different, although device structure of red and green devices and the LUMO energy level of Ir(ppy)$_3$ and Ir(pq)$_2$(acac) are same. The hole injection barrier from NPB into emission layer is relatively high as 0.4 eV. In this case, holes prefer to be directly injected into HOMO of dopant rather than host. The hole injection from NPB into Ir(ppy)$_3$ with hole injection barrier of 0.1 eV is easier than that from NPB into Ir(pq)$_2$(acac) with hole injection barrier of 0.3 eV. Therefore, operating voltage of green device is slightly lower than that of red device. Moreover, we compared the current density property of CBP and LPGH 153 in green device, as shown in Figure 3 and inset of Figure 3. The current density of green device with LPGH 153 is very high compared with that with CBP because of the efficient electron transport ability of LPGH 153 as confirmed in electron only device. It can improve the charge balance of hole and electron in organic semiconductor that electron mobility is lower than hole mobility. The leakage current of device with LPGH 153 is very low as shown in inset of Figure 3. The leakage current of green device with CBP was located between $10^{-5}$ mA/cm$^2$ and $10^{-6}$ mA/cm$^2$. On the other hand, the leakage current of green device with LPGH 153 was located between $10^{-6}$ mA/cm$^2$ and $10^{-7}$ mA/cm$^2$, implying the amorphous LPGH 153 film with a surface roughness less than 1 nm is relatively free from the formation of pin hole as comparison with CBP film under the driving of device.

The luminous efficiency and external quantum efficiency of red and green devices with LPGH 153 are shown in Figure 4 and inset of Figure 4, respectively. The maximum luminous efficiencies are obtained as 22.2 cd/A and 32.2 cd/A for the red and green devices, respectively. And the red and green devices have the maximum external quantum efficiencies of 14.1% and 9.3%, respectively. The different tendency between luminous efficiency and external quantum efficiency results is because that the luminous efficiency is regardless of the eye sensitivity of human, while the external quantum efficiency is associated with that. As a result, the absolute efficiency of LPGH 153 regardless of human eye sensitivity is superior in red

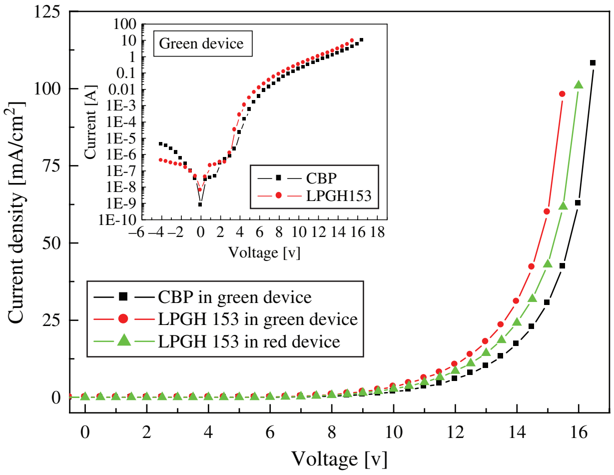

**Fig. 3.** Current density–voltage characteristics of red and green phosphorescent OLEDs with LPGH 153. The current density of green device with LPGH 153 was also compared with that of the green device with CBP host. (inset; log-scale).

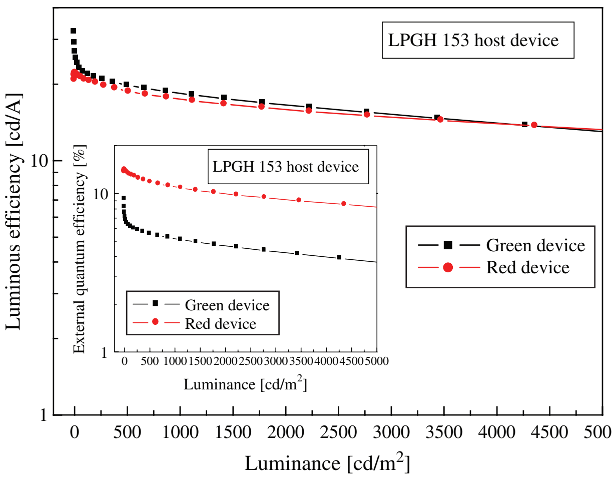

**Fig. 4.** Luminous efficiency (inset; external quantum efficiency) of red and green phosphorescent OLEDs with LPGH 153.

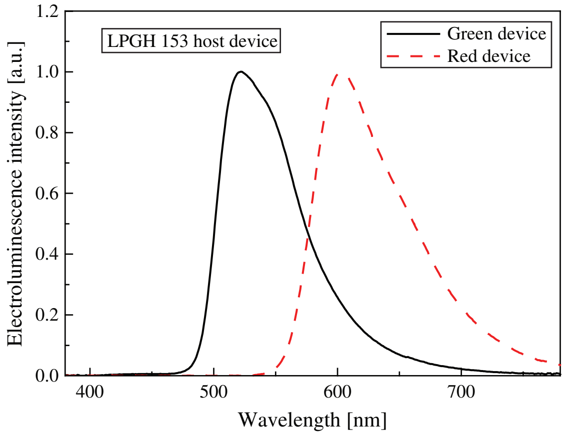

**Fig. 5.** Normalized EL spectra of red and green phosphorescent OLEDs with LPGH 153 as a host at applied voltage of 8 V.

device rather than in green device. It is because the energy band of Ir(pq)$_2$(acac) is relatively more narrow than that of Ir(ppy)$_3$. Therefore, the energy transfer from LPGH 153 into Ir(pq)2(acac) is more efficient than that from LPGH 153 into Ir(ppy)$_3$ and the leakage of excitons formed in Ir(pq)$_2$(acac) can be relatively suppressed as comparison with that in Ir(ppy)$_3$.

The electroluminescence (EL) spectra of red and green devices with LPGH 153 are shown in Figure 5. The red and green devices showed typical EL spectra of Ir(pq)$_2$(acac) and Ir(ppy)$_3$, respectively. The peaks maximum of the EL spectra was observed at about 603 nm and 523 nm for the red and green devices, respectively. There was no charge leakage out of the emitting layer and only emission from the dopant material was obtained. Therefore, it can be concluded that charge confinement and charge balance in the devices with LPGH 153 are responsible for the improved efficiency in the devices with LPGH 153.

## 4. CONCLUSION

In summary, a novel carbazole-type LPGH 153 is effective as red and green phosphorescent host. A high luminous efficiencies 22.2 cd/A and 32.2 cd/A were obtained in red and green devices, respectively, due to a wide HOMO-LUMO bandgap of 3.2 eV for efficient energy transfer and a charge balance in the light-emitting layer. The LPGH 153 also showed a smooth surface morphology with an average surface roughness less than 1 nm and leaded to few leakage current compared with CBP. Therefore, the LPGH 153 is promising as a host in red and green phosphorescent OLEDs.

**Acknowledgment:** This work was supported by Energy Resources Technology Development program (No. 2007-E-CM11-P-07) and Strategy Technology Development program (No. 10030834) from Ministry of Knowledge Economy (MKE). Moreover, this research was also supported by the ERC program of the Korea Science and Engineering Foundation (KOSEF) grant funded by the Korea Ministry of Education, Science and Technology (MEST) (No. R11-2007-045-03001-0).

## References and Notes

1. J. H. Kim, M. C. Choi, H. J. Kim, Y. K. Kim, J. H. Chang, M. J. Han, I. I. Kim, and C. S. Ha, *J. Nanosci. Nanotechnol.* 10, 388 **(2010)**.
2. H. C. Park, J. W. Park, and S. G. Oh, *J. Nanosci. Nanotechnol.* 9, 7260 **(2009)**.
3. M. A. Baldo, D. F. O'Brien, Y. You, A. Shoustikov, S. Sibley, M. E. Thompson, and S. R. Forrest, *Nature* 395, 151 **(1998)**.
4. D. F. O'Brien, M. A. Baldo, M. E. Thompson, and S. R. Forrest, *Appl. Phys. Lett.* 74, 442 **(1999)**.
5. C. Adachi, M. A. Baldo, S. R. Forrest, S. Lamansky, M. E. Thompson, and R. C. Kwong, *Appl. Phys. Lett.* 78, 1622 **(2001)**.
6. Y. Kawamura, S. Yanagida, and S. R. Forrest, *J. Appl. Phys.* 92, 87 **(2002)**.
7. A. Tsuboyama, H. Iwawaki, M. Furugori, T. Mukaide, J. Kamatani, S. Igawa, T. Moriyama, S. Miura, T. Takiguchi, S. Okada, M. Hoshino, and K. Ueno, *J. Am. Chem. Soc.* 125, 12971 **(2003)**.
8. M. A. Baldo, M. E. Thompson, and S. R. Forrest, *Pure Appl. Chem.* 71, 2095 **(1999)**.
9. J. Y. Lee, *Appl. Phys. Lett.* 89, 223517 **(2006)**.
10. T. Tsuji, S. Kawami, S. Miyaguchi, T. Naijo, T. Yuki, S. Matsuo, and H. Miyazaki, *SID Int. Symp. Digest Tech. Paper* 35, 900 **(2004)**.
11. K. Kanno, K. Ishikawa, Y. Nishio, A. Endo, C. Adachi, and K. Shibata, *Appl. Phys. Lett.* 90, 123509 **(2007)**.
12. A. J. Bard and L. R. Faulkner, Electrochemical Methods, Fundamentals and Applications, John Wiley & Sons, New York **(1980)**.

Received: 1 November 2009. Accepted: 1 April 2010.